BEAM LOSS STUDIES FOR THE P42 BEAMLINE AT THE CERN SPS NORTH AREA

L. A. Dyks*, C. Ahdida, D. Banerjee, A. Baratto Roldan, J. Bernhard, M. Brugger, N. Charitonidis, M. Fraser, L. Gatignon, A. Goillot, M. A. Jebramcik, E. Nowak, G. Mazzola, F. Metzger, R. Murphy, L. J. Nevay, E. G. Parozzi, B. Rae, S. Schuh-Erhard, F. Stummer, M. Van Dijk
CERN, 1211 Meyrin, Switzerland

Abstract

The P42 beamline transports 400 GeV protons from the CERN SPS between the T4 and T10 targets. A secondary particle beam is produced at the T10 target and transported along the K12 beamline to the experimental cavern ECN3, presently housing the NA62 experiment. In the context of the Physics Beyond Colliders (PBC) study, an increase of the beam intensity in P42 has been considered to provide protons to a future high-intensity fixed-target experiment in ECN3. For both its present usage and especially for the intensity upgrade, it is important to reduce beam losses to a minimum to decrease radiation levels and protect equipment. In this study, simulations of P42 with the Monte Carlo software BDSIM, are used to demonstrate that beam losses in P42 are primarily driven by particle-matter interactions in material intercepted by the beam. The distribution of the simulated losses is compared to doses measured along the beamline in radiation protection surveys and beam loss monitors. Future mitigation strategies to reduce beam losses are then discussed and evaluated.

INTRODUCTION

The ECN3 experimental cavern, part of the CERN North Area (NA) [1], has hosted a number of fixed-target experiments since the 1970s, with the NA62 kaon experiment, presently installed [2].

As part of the Physics Beyond Colliders (PBC) study [3] it has been proposed to increase the intensity of the proton beam heading to ECN3. The high-intensity ECN3 project (HI-ECN3) was set up to explore the feasibility of this and to explore the physics potential [4, 5], leading to the approval of the Search for Hidden Particles experiment (SHiP) in 2024 [6]. The goal of SHiP is to search for feebly interacting particles and thus requires as many protons on target as possible. Each spill is due to contain a maximum intensity of 4×10^{13} protons compared to 3×10^{12} protons for nominal NA62 operation. Therefore, substantial work is ongoing to improve beam delivery to ECN3 with a key element being to understand and mitigate beam losses in P42.

Beamline Description

P42 transports protons from T4 to the T10 target. T4 consists of five Be plates of lengths 40 - 500 mm, each of which can be placed into the beam to produce secondary particles for the H6 and H8 beamlines, and if requested P42, absorbing some of the proton beam. Beam sharing between P42, H8 and H6 is done using dipoles placed either side of T4 [7], known as wobbling magnets, to vary the horizontal incidence angle on the target. Target beam instrumentation monitors (TBIU/D) are installed upstream and downstream of T4. Following the final wobbling magnets, there is a 6.6 m long, 900 mm diameter vacuum chamber (VXSS), before two target attenuator (TAX) collimators, designed to capture undesired secondary and scattered particles produced in T4. Installed in air, each TAX is made from 4, 0.4 m long metal blocks, with holes of different dimensions through them. Each TAX can be independently moved to select different holes. Additional fixed (TCX) and 4-block movable collimators, XCHV, are installed downstream. The P42 optics are discussed in [8]. For this study it should be noted that the beam size is large relative to the aperture in the horizontal axis at $s = 170$ m and $s = 400$ m where the magnitude of horizontal dispersion is also large, and large relative to the vertical aperture in bend 7 ($s \sim 550$ m) and at Q20 ($s \sim 800$ m).

BEAM LOSSES

Following the restart of operation after Long Shutdown 2 (LS2) in 2021, substantially higher losses were measured than before [9]. Elevated radiation levels were locally measured outside the transfer tunnel at two shielding weaknesses along P42, namely at an access ramp ($s \sim 600$ m) and a road bridge ($s \sim 800$ m), increased activation levels of the beamline elements were found (Fig. 1), and the transmission from T4 to T10 was reduced. The beam spot at T10 was also significantly larger than before LS2. Work was done to identify the cause of the losses [5], such as reducing the amount of material in the beamline, improving the alignment of components [10], and investigating the optics [8]. Further work was done to mitigate their impact by installing improved shielding below the ramp. To actively measure beam losses, 13 beam loss monitors (BLM) were installed [11].

During the Year End Technical stop in 2022, the dominant cause of the additional losses was discovered. The supports for the VXSS vacuum chamber had failed causing the chamber to move by several cm. The beam subsequently passed through the 22 mm thick stainless steel end cap rather than the 200 μm Al vacuum window, resulting in significant scattering. Due to the location of the VXSS, the scattered particles were not collimated efficiently by the TAX. The VXSS was removed in 2023, significantly reducing beam losses. As shown in Fig. 1, the measured contact ambient dose equivalent rate H*(10), scaled to the same cooldown time, was up to a factor ~ 5 to 10 lower in 2023 than 2022.

* Corresponding author: luke.dyks@cern.ch

The largest improvement in activation is at the XCHV at 286 m, as it was necessary to use this to collimate the beam in 2022 to reduce dose rates at the local shielding weaknesses. There is little reduction in activation following the horizontal bend, bend 7, just before the ramp at $s \sim 520$ m to 560 m.

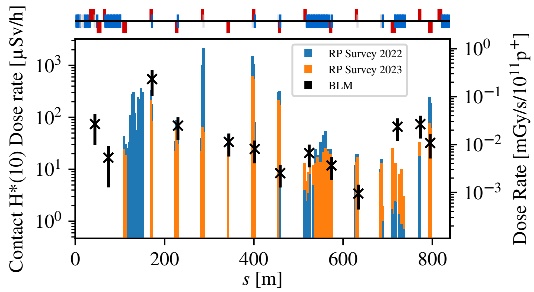

Figure 1: Residual ambient dose equivalent rate H*(10) measured at contact after operation in 2022 and 2023, and the average prompt absorbed dose rate measured by BLMs during 2023 normalised by the intensity on T10 vs. s.

Despite the reduction in activation there are still losses. The average dose rate measured by the BLMs in 2023 is shown in Fig. 1. It is difficult to compare the signal of each BLM to activation in the same location for several reasons; each BLM will be closer or further away from the source of losses in a particular region; different amounts of material are between the source and BLM which act as shielding; and different operation scenarios result in losses in different locations varying through the year. However, there are some similarities such as the maximum BLM signal and activation both occurring at 170 m.

There are several possible causes of the losses, such as an optics mismatch. However, during optics studies it was not possible to reduce losses below a baseline. The losses could also be caused by scattering with material in P42. Inelastic scattering processes between a proton and material reduce the energy of the proton and produce secondary particles. These are not likely to be transported far downstream. However, a proton that undergoes elastic, or quasi-elastic scattering receives a kick in angle but could be transported to a point further downstream where it impacts the aperture.

Table 1: Material present in the P42 Beamline

Element	s [m]	Material	N_{λ_I} [10^{-3}]
Window 1	−1.15	Al	1.26
TBIU/D	−0.53 & 0.48	Ti + Al	2.64
Air - T4	0	Air	2.34
Window 2	1.10	Al	0.50
Win. VXSS	16.61	Al	0.50
Air - TAX	16.61 - 20.60	Air	5.34
Window 3	20.60	Al	0.50

The T4 target is evidently a source of beam scattering. However, losses are not seen to change significantly along P42 when a longer target plate is used or the target removed. Additionally, the beam to future HI-ECN3 will bypass the target, only moving through the air and TBIU/D in the T4 region. Material, other than the target, present in the first 25 m of P42 and the number of nuclear interaction lengths through that material, N_{λ_I}, are listed in Tab. 1. It should be noted that as the VXSS was removed in 2023, a further ~ 7 m of air is present in the beamline beginning at $s \sim 9.6$ m, with a vacuum window equivalent to the VXSS window installed at this location. The VXSS is due to be replaced in Long Shutdown 3. Secondary emission monitors, made from thin metal foils can also scatter the beam but are installed on in-out motors. The only other material in P42 is the vacuum window and TBIU before T10. The vacuum level in P42 is $\sim 10^{-3}$ mbar, which does not result in significant losses [12].

The largest source of interactions on the HI-ECN3 beam is material in the region around T4. However, there is a rotation in phase-space between T4 and the TAX to collimate any protons scattered around T4. The only other large source of beam scattering is the air inside the TAX itself. Any particle scattered in this region is less likely to be collimated by the TAX thus could be transported downstream.

BDSIM SIMULATIONS

To investigate the impact of scattering on the losses in P42, Monte Carlo simulations were performed using BDSIM (version `1.7.4`, Geant4 version `10.7.2.3-ftfp-boost`) [13, 14]. A full model of P42 was produced from the MADX model [15, 16], with accurate models of the beamline elements. Field maps inside the magnet yokes were generated for a generic magnet geometry by BDSIM. The optics and tracking were validated by simulating 50000 protons through P42 without particle interactions, and showed good agreement. The simulations begin 0.1 m before window 1 using a beam distribution generated from the Twiss parameters calculated in MADX for the dedicated HI-ECN3 beam. In each case discussed, 1 million protons were simulated using the Geant4 reference physics list `FTFP_BERT` and all particles produced above a kinetic energy 0.5 GeV were tracked.

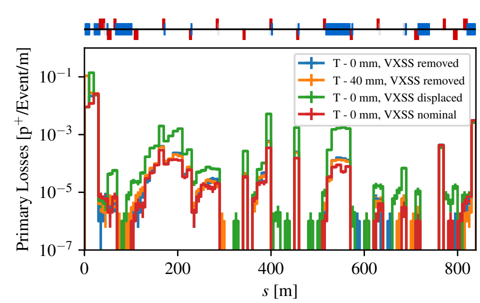

Figure 2: Primary proton losses vs. s for scenarios comparing operation in 2022 and 2023.

Geant4 primary losses are shown in Fig. 2 for the beamline in 2022, with the VXSS end-cap in the beam, and for 2023, with the VXSS removed. 14 mm and 12 mm holes were used in the TAX. The distribution of losses is similar to the activation shown in Fig. 1 for both years. The maximum losses occur in regions where activation is high, namely at 170 m and 400 m. There is an order of magnitude reduction in losses when the VXSS is removed, even in bend 7, which is not seen in the activation levels. Including a target does not increase losses, except in the first ~ 200 m. When the VXSS is placed back in its nominal location the losses are even lower. However, this difference is about 5 times smaller than the difference shown in Fig. 2.

Scattered particles can be grouped into two separate categories: a halo, from elastic collisions, and an energy tail coming from inelastic collisions. Particles in the halo can be lost at aperture restrictions. As the beam travels along P42 the halo becomes depleted. In 2022, the XCHV at 286 m was used to collimate the halo produced in the VXSS in the vertical plane, which could explain why the difference in activation between 2022 and 2023 was so small in bend 7, as this is a location where losses are due to the vertical halo.

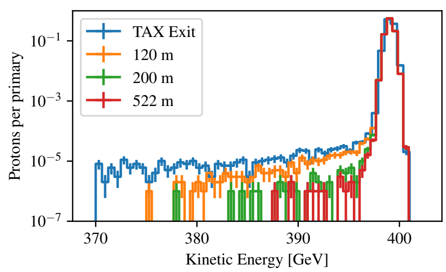

Figure 3: Proton kinetic energies at different s along P42, simulated with the VXSS removed and no T4 target.

An example of the proton kinetic energy distribution at different distances along P42 is shown in Fig. 3. A low-energy tail, produced in multiple locations, is able to pass through the TAX. As the beam moves along P42 the tail is lost. The majority of the tail is lost approaching the first dispersion maximum, ~ 170 m. Following the second maximum, ~ 400 m, the tail is effectively collimated and produces few further losses. The magnitude of this tail increases with target length due to additional inelastic collisions leading to higher losses before s = 170 m for longer targets.

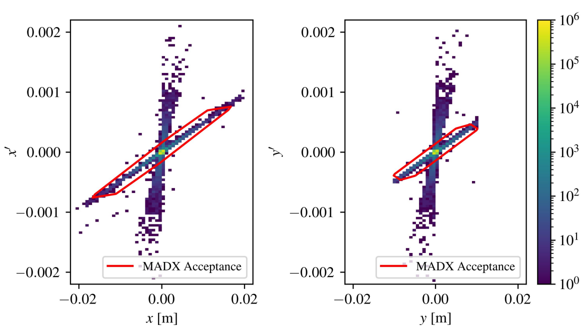

Figure 4: Trace-space in x and y for a pencil beam tracked to window 3, following the TAX, in BDSIM with the acceptance to T10 calculated in MADX overlaid.

To understand the relative effect of different material on losses, simulations were done for a pencil beam of no spatial, angular, or momentum spread. Particles that deviate from the beam core in trace-space can only do so through scattering. The trace-space of protons of momentum greater than 397 GeV/c from a pencil beam simulated to 20.6 m, is shown in Fig. 4. All beamline material was included, with no target plate, the VXSS chamber placed in the nominal location, and both TAX holes set to 40×20 mm^2. There are two distinct regions of the halo, one created in the T4 region and one in the TAX. Particles scattered to large angles in the T4 region have a large spatial spread at the TAX and are collimated. Whereas, particles scattered in the TAX are mostly not collimated. By back-tracking the P42 apertures in MADX to this location, using the method outlined in [17], it is possible to overlay the acceptance of P42 on the trace-space. The air in the TAX scatters a large number of protons out of the acceptance, and is, therefore, the dominant source of losses. Whereas most particles scattered within the T4 region that pass through the TAX are within the acceptance. Losses from the T4 region are predominantly from lower momentum protons and are concentrated in the early part of the beamline. The losses along P42 for this pencil beam are shown in Fig. 5. The distribution of losses is almost identical to the physical beam shown in Fig. 2, implying that large-angle scattering is the predominant driver of losses and not a small-angle emittance blowup.

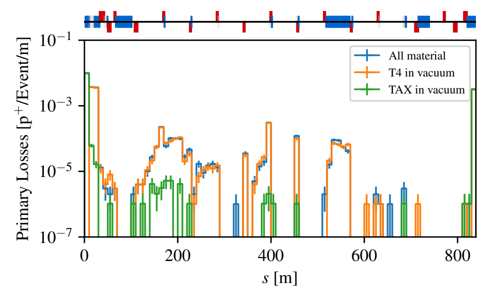

Figure 5: Primary proton losses vs. s for a pencil beam simulated with different material present in P42.

If the TAX was modified to create a continuous vacuum from window 2 to T10, losses could be substantially reduced. Simulated losses for that scenario are shown in Fig. 5. As a comparison simulated losses are also shown for a scenario where the TAX is left as presently installed but only the T4 region is placed in vacuum. Installing vacuum at T4 makes almost no difference to the simulated losses. The opposite is the case for an modified TAX where the losses are reduced by over an order of magnitude. The in-vacuum TAX still collimates particles scattered in T4, but does not drive significant losses itself. The feasibility of such an upgrade should be investigated, whilst respecting the use of the TAX as a safety element. If it is not possible to upgrade the TAX in this way, then local shielding, and if necessary, a collimation system should be investigated.

CONCLUSIONS

Simulations of P42 with BDSIM have improved the understanding of beam losses in P42. The dominant source of beam losses, namely the air in the TAX, has been identified and work is ongoing to reduce these. The BDSIM model of P42 is being improved to include more realistic magnet field maps and to model the response of radiation monitors such as the BLMs. Additionally, the model will be used to optimise the future design of P42 for HI-ECN3 and SHiP and make sound design choices.

REFERENCES

[1] D. Banerjee *et al.*, "The North Experimental Area at the Cern Super Proton Synchrotron," 2021. doi:10.17181/CERN.GP3K.0S1Y

[2] E. Cortina Gil *et al.*, "The Beam and detector of the NA62 experiment at CERN," *Journal of Instrumentation*, vol. 12, no. 05, P05025, 2017. doi:10.1088/1748-0221/12/05/P05025

[3] J. Beacham *et al.*, "Physics beyond colliders at CERN: beyond the Standard Model working group report," *Journal of Physics G: Nuclear and Particle Physics*, vol. 47, no. 1, p. 010 501, 2019. doi:10.1088/1361-6471/ab4cd2

[4] C. Ahdida *et al.*, "Post-LS3 Experimental Options in ECN3," CERN, Tech. Rep., 2023. https://cds.cern.ch/record/2867743

[5] C. Ahdida *et al.*, "Findings of the Physics Beyond Colliders ECN3 Beam Delivery Task Force," CERN, Tech. Rep., 2023. https://cds.cern.ch/record/2847433

[6] O. Aberle *et al.*, "BDF/SHiP at the ECN3 high-intensity beam facility," CERN, Tech. Rep., 2022. https://cds.cern.ch/record/2839677

[7] L. Gatignon, "Design and Tuning of Secondary Beamlines in the CERN North and East Areas," 2020. doi:10.17181/CERN.T6FT.6UDG

[8] L. Dyks *et al.*, "Characterisation of the optics of the TT24 and P42 beam lines in the CERN SPS north area," presented at IPAC'24, Nashville, TN, USA, May 2024, paper TUPC74, this conference.

[9] J. Bernhard, L. Gatignon, and N. Doble, "Recent Studies on Radiation at the Ramp to EHN1 from the P42 Beam," CERN, Tech. Rep., 2023. https://edms.cern.ch/document/2816855

[10] C. Vendeuvre and V. Kyrgiannaki, "P42 Alignment Campaign," CERN, Tech. Rep., 2023. https://edms.cern.ch/document/2927202

[11] J. Bernhard, M. Fraser, R. Ramjiawan, F. Roncarolo, A. Lafuente, and L. Krzempek, "Installation of Additional Beam Profile Monitors (BSG) in the North Area P42 Primary Line," CERN, Tech. Rep., 2023. https://edms.cern.ch/document/2777725

[12] L. Dyks, M. Fraser, and M. Santos, "Vacuum System of the P4/P42 Primary Beamline for the High Intensity Facility in ECN3," CERN, Tech. Rep., 2024. https://edms.cern.ch/document/3006552

[13] L. Nevay *et al.*, "BDSIM: An accelerator tracking code with particle–matter interactions," *Computer Physics Communications*, vol. 252, p. 107 200, 2020.

[14] J. Allison *et al.*, "Recent developments in Geant4," *Nuclear Instruments and Methods in Physics Research Section A: Accelerators, Spectrometers, Detectors and Associated Equipment*, vol. 835, pp. 186–225, 2016. doi:https://doi.org/10.1016/j.nima.2016.06.125

[15] *Methodical accelerator design X*, https://madx.web.cern.ch/madx, 2024.

[16] *P42 MADX*, https://gitlab.cern.ch/acc-models/acc-models-ea.

[17] A. Baratto-Roldán, M. Perrin-Terrin, E. G. Parozzi, M. A. Jebramcik, and N. Charitonidis, *NuTag: proof-of-concept study for a long-baseline neutrino beam*, Submitted to EPJ-C, 2024. arXiv:2401.17068